

ChemBioChem

Supporting Information

Core-Shell DNA-Cholesterol Nanoparticles Exert Lysosomolytic Activity in African Trypanosomes**

Robert Knieß[†], Wolf-Matthias Leeder[†], Paul Reißig, Felix Klaus Geyer, and H. Ulrich Göringer*

Table of Contents

1	SI Tables and Figures
1.1	Table S1
1.2	Figure S1
1.3	Figure S2
1.4	Figure S3
1.5	Figure S4
1.6	Figure S5
1.7	Figure S6

1 SI Tables and Figures







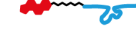


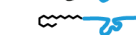
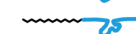







cartoon depiction	designation	length (nt)	nucleic acid	lipid modification	attachement site	linker chemistry	antiSL-DNAzyme sequence	aggregation number	cmc monomer concentration (nM)	LC ₅₀ micelle concentration (nM)
	Dz39	39	DNA	none	none	none	+	none	none	non-toxic
	Dz39_5'-Chol-Pro	39	DNA	cholesterol	5'	pro	+	n.d.	13	67
	Dz39_3'-Chol-TEG	39	DNA	cholesterol	3'	TEG	+	28	116	79
	Dz39_3'-Chol-Pro	39	DNA	cholesterol	3'	pro	+	33	42	33
	D39rand_3'-Chol-Pro	39	DNA	cholesterol	3'	pro	-	n.d.	112	51
	Dz31	31	DNA	none	none	none	+	none	none	non-toxic
	Dz31_5'-Chol-Pro	31	DNA	cholesterol	5'	pro	+	30	46	79
	Dz31_3'-Chol-Pro	31	DNA	cholesterol	3'	pro	+	69	148	62
	D31rev_3'-Chol-Pro	31	DNA	cholesterol	3'	pro	-	n.d.	42	64
	Dz31_5'-Oleate	31	DNA	oleate	5'	pro	+	n.d.	none	non-toxic
	Dz31_5'-Stearyl	31	DNA	stearyl	5'	pro	+	n.d.	none	non-toxic
	D20	20	DNA	none	none	none	-	none	none	non-toxic
	D20_3'-Chol-Pro	20	DNA	cholesterol	3'	pro	-	42	112	79
	R20_3'-Chol-Pro	20	RNA	cholesterol	3'	pro	-	n.d.	87	178
	D20PTO_3'-Chol-Pro	20	PTO	cholesterol	3'	pro	-	n.d.	330	136
	D10	10	DNA	none	none	none	-	none	none	non-toxic
	D10_3'-Chol-Pro	10	DNA	cholesterol	3'	pro	-	39	151	162
	D6_3'-Chol-Pro	6	DNA	cholesterol	3'	pro	-	30	94	182

Table S1. Cartoon representation and data summary of all synthesized oligonucleotides and DNA/RNA-lipid conjugates. DNA and RNA sequences are depicted as lines in cyan (DNA), purple (RNA), and green/yellow (phosphorothioate (PTO)-modified DNA). The presence of the SL-DNAzyme is indicated by an outline of the 2D structure. Cholesterol modifications are in red. The individual sequences of the different constructs are listed in the experimental section of the manuscript. Table S1 includes the micellar aggregation number, the critical micelle concentration (CMC), and the half-maximal lethal concentration (LC₅₀) for infective stage trypanosomes. TEG =triethylene glycol. pro=prolinol. n.d.=not determined.

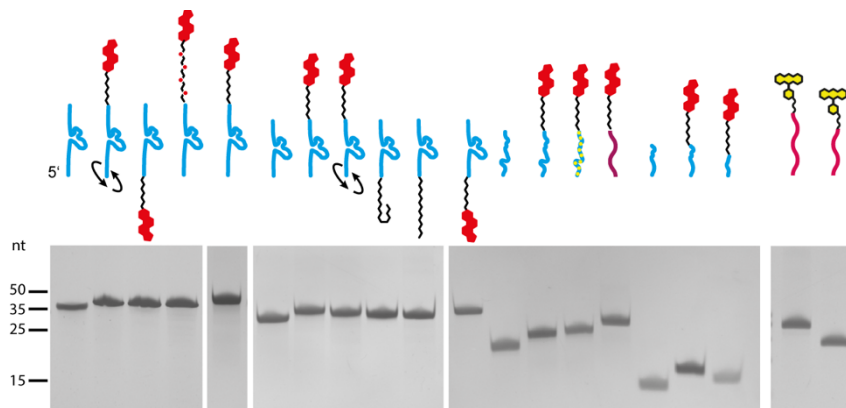


Figure S1. Quality control of chemical synthesis. Gel electrophoretic separation of all synthesized DNA-lipid conjugates, RNA-lipid conjugates, and SL-RNA-mimicking oligoribonucleotides in urea-containing (8M) 18% (w/v) polyacrylamide gels. Purities are $\geq 97\%$. For a summary of the molecule drawings see Supporting information Table S1.

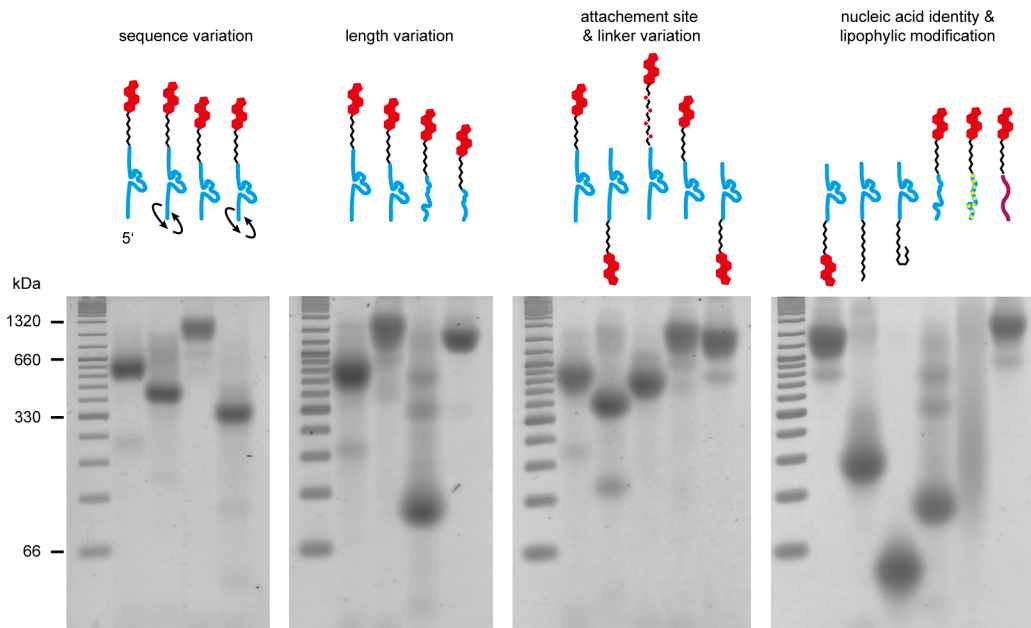


Figure S2. High molecular mass nanoparticle formation of different DNA- and RNA-lipid conjugates analyzed in non-denaturing 3% (w/v) agarose gels. The different constructs are grouped (left to right) according to their sequence and length variation, the 5'- or 3'- attachment of the cholesterol moiety, the variation in linker chemistry (prolinol *versus* TEG), the nucleic acid identity (DNA, RNA, PTO-modified DNA) and the lipophilic side group (cholesterol, oleate, stearate). For a summary of the molecule drawings see Supporting information Table S1.

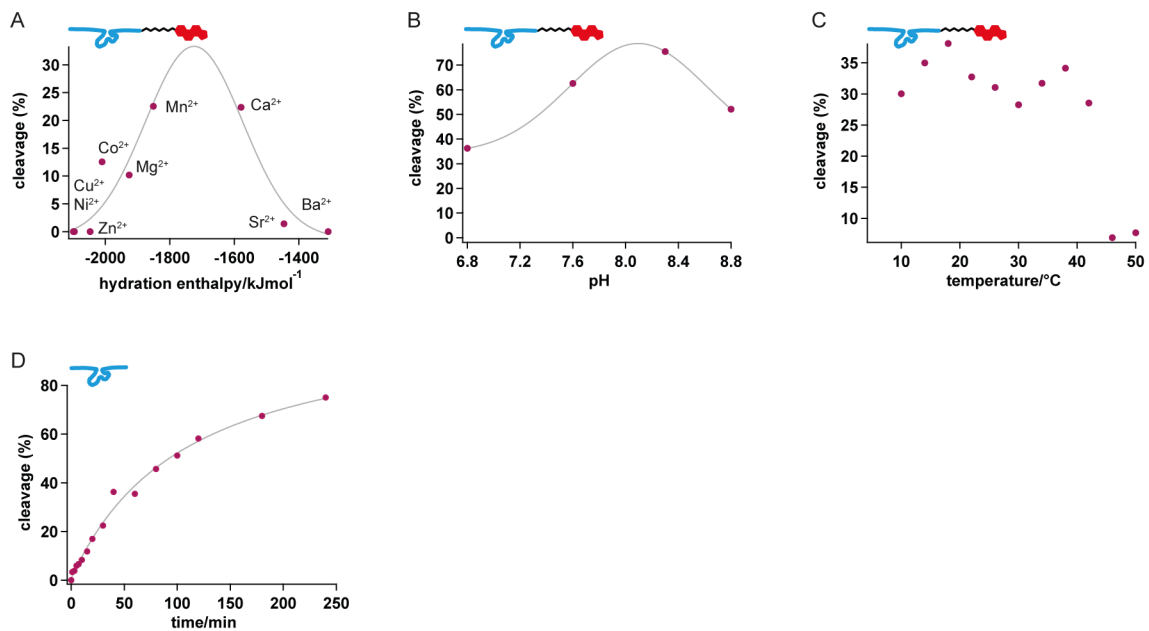


Figure S3. Characteristic features of the SL-RNA-specific DNAzyme. (A) Divalent cation dependency. (B) pH-optimum. (C) Temperature optimum. (D) Single turnover kinetics at a 5x molar excess of the SL-DNAzyme over SL-RNA substrate. Up to 80% of input SL-RNA is cleaved after 4h of incubation. $k_{cat}=0.01/\text{min}$.

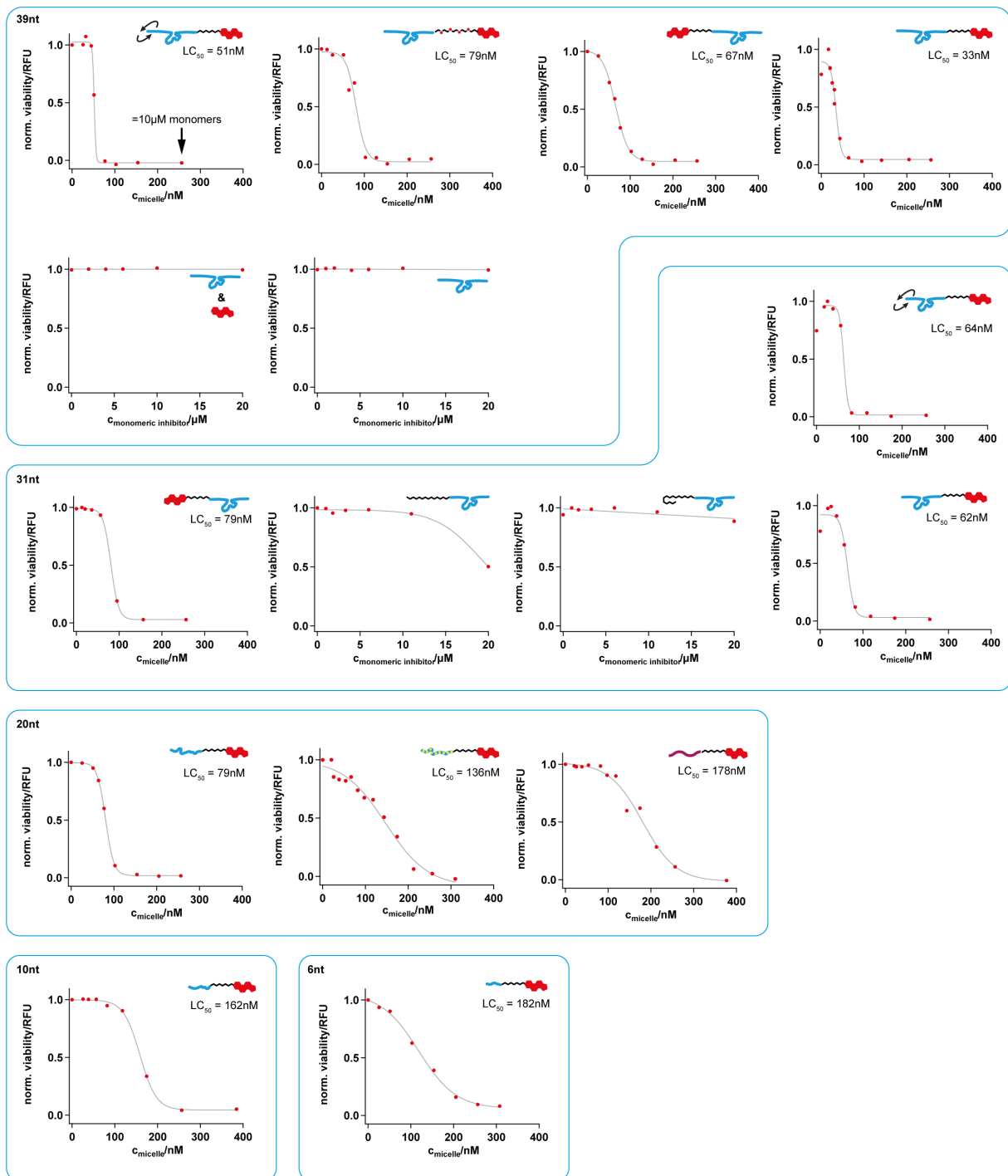


Figure S4. Dose-response curves and LC_{50} -values of infective-stage trypanosomes treated with different DNA-lipid nanoparticles. The various plots are grouped according to the nucleotide length of the DNA/RNA domain of the nanoparticle constructs. Molecule drawings are listed in Supporting information Table S1. RFU=relative fluorescence unit.

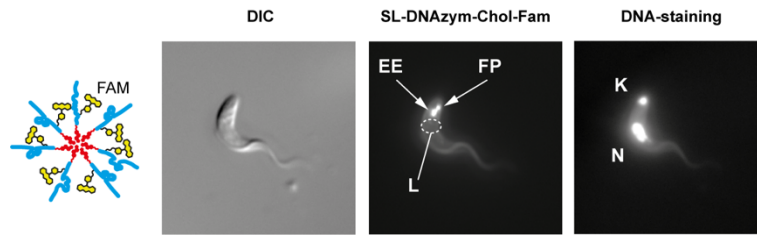


Figure S5. Early events in the trypanosome/DNA-cholesterol nanoparticle interaction. Left: Differential interference contrast (DIC) imaging. Center: Fluorescence imaging (FAM). Right: DNA staining. N=nuclear DNA. K=kinetoplast DNA. FP=Flagellar pocket. EE= Early endosome. L=Lysosome. The picture shows binding of a FAM-labelled SL-DNAzyme-cholesterol nanoparticle to the flagellar pocket (proximal to the kinetoplast) and internalization of the particle into early endosomes (EE). Please note that at this point no signal in the lysosome is detectable. For a comparison to time points >2h see Figure 6B.

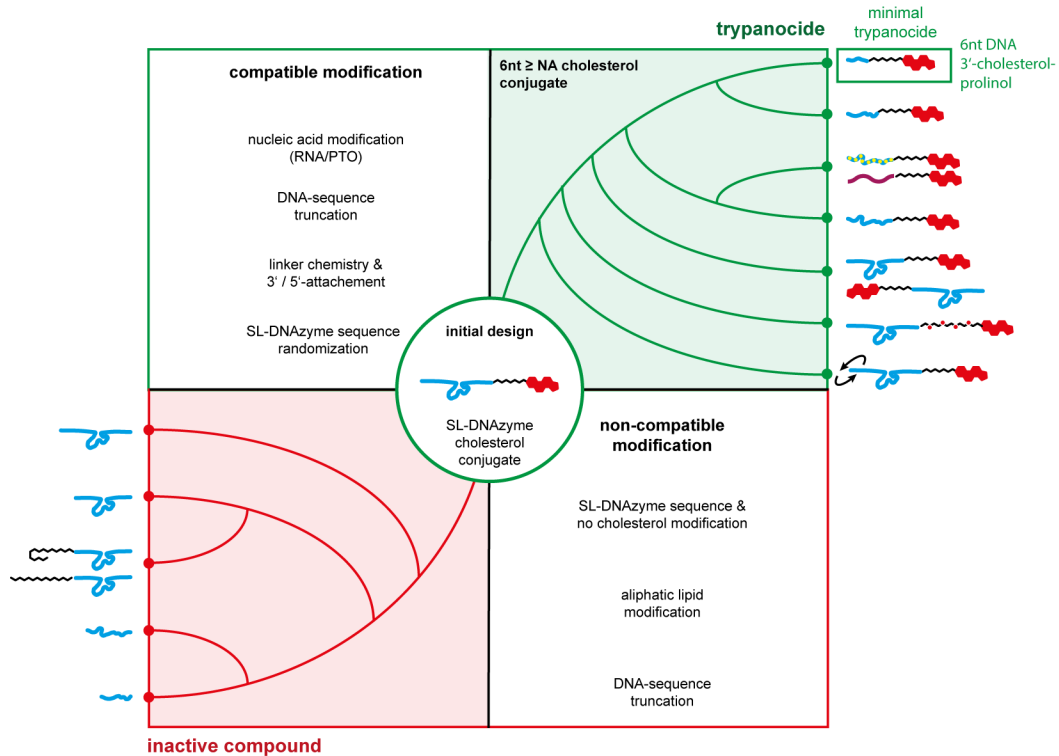


Figure S6. Summary of compatible and noncompatible modifications and characteristics for the synthesis of DNA-cholesterol nanoparticles with trypanocidal activity.